

Measurement and Investigation of PCC Point Harmonics in a Grid-tied PV Station

Ravina Raut, 2Prof. Ganesh Wakte 1M. Tech. Student (PG), 2Assistant Professor,

Electrical Engineering Department, Abha Gaikwad College of Engineering Nagpur, India

Abstract-This paper addresses the PCC-point harmonics in a parallel-inverter-based photovoltaic station. Firstly, the harmonic measurement of a grid-tied PV station has been implemented. The voltage and current waveforms present some significant characteristics, such as lower frequency, power correlation and inter-harmonic. The most of these harmonic currents flows through the inverter IGBT bridges and filter inductance branches, rather than the filter capacitor branches. These harmonics are 3-phase symmetric and contain 3rd and 6th harmonic components. These harmonics are not produced by the resonances related to the output LCL filters of PV inverters. This study proposes that the resonances between inverter and grid impedance are the dominant causes of the harmonics.

Keywords-Harmonic resonance, Serial resonance, Grid-tied PV, PV inverter, Self-oscillation

I. INTRODUCTION

The power industry is experiencing structural changes as more distributed generation units are integrated into low-voltage power distribution systems[1-3]. These distributed generation units are used to deliver renewable and clean energy such as photovoltaic power, wind power, and fuel cell power, to the utility grid through interfacing inverters[4-5]. Previous research on grid-connected inverters mainly focused on load demand sharing during micro-grid islanding operation[6]. In practice, each inverter of microgrid is assumed to be decoupled from other inverters with the stiff point of common coupling (PCC) voltage[7-8]. However, this model cannot describe the complex resonances among parallel-inverter units because of the higher up-stream grid impedance of microgrid. In [9], a simplified passive circuit model was presented to investigate the resonances in microgrid. In [10], the interaction of parallel inverters based on the open-loop transfer function matrix has been discussed.

Recently, more and more types of improved methods have been reported to address the LCL filter resonance[11]. In general, these model-based control methods are sensitive to system parameter variations and consider only the impedance of passive filter component. The control scheme should account for the effects of inverter control on the output impedance and harmonic

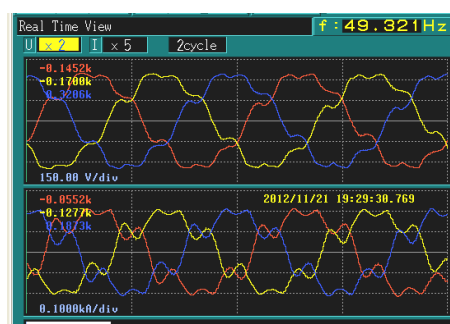
emission. The influence of control function should not be ignored. This paper presents field measurement results of PCC to demonstrate the multiple harmonic resonances. The goal of the research is to reveal the main causes of PCC harmonic at PV connected-point in a micro-grid.

II. CHARACTERISTICS OF PCC HARMONICS

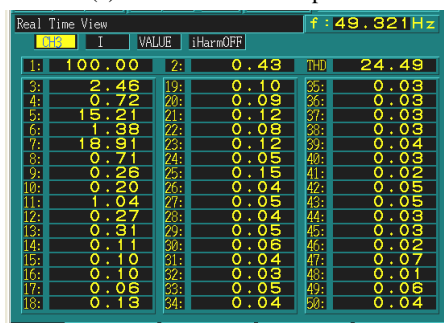
To demonstrate the PCC harmonics of multiple grid-connected inverters, an isolation microgrid consists of hydroelectricity and photovoltaic is addressed. The capacity of hydroelectricity in microgrid is 12.8MW and, the capacity of photovoltaic of PV is 2MW. The capacity of each inverter in PV station is 100KVA and the amount of inverters is 20.

Every inverter uses a standard current-source converter (CSC) topology with an inductive output filter. The filter capacitor is 47×10^{-6} F. The groups consisting of 3-6 parallel inverters are connected to PCC of the microgrid. Five grid-tied transformers between inverter groups and microgrid are installed to interface 10KV/400V buses. The isolating transformer of each inverter is 400V/215V. The controller of inverter is PI regulator in the dq reference frame. The batteries in PV generation branches decouple the grid-tied inverters and the photovoltaic sections completely. The CSC inverters are working at an ideal condition of DC sides and the research can focus on the harmonics occurring at PCC point.

Operation of the inverters under different output power conditions has been measured. The measured waveforms, both of voltage and current at PCC by power quality analyzer, are presented in Fig. 1 when the output power is 0.8MW. The main components of harmonics are 5th and 7th (15.2% and 18.9% respectively), and the THD is 24.5%. The waveforms of 3-phase voltages and currents are not symmetrical perfectly, indicating that there are inter-harmonics at PCC.



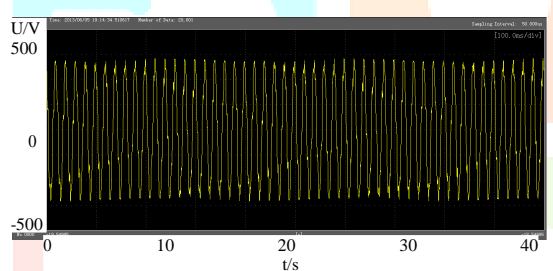
(a) Waveforms at PCC point



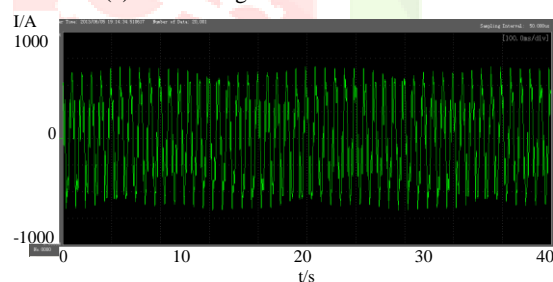
(b) Value lists of PCC harmonics

Fig. 1. Harmonic measurement by Power Quality Analyzer

To further characterize the harmonics, the waveform recording had been implemented by waveform recorder as Fig. 2 and the waveform data were analyzed using Fourier Transforms.



(a) PCC voltage waveforms vs. time



(b) PCC current waveforms vs. time

Fig. 2. PCC waveforms of a PV station

The dominate frequency components of PCC voltage harmonics in a measurement period (lasting 39s) are presented as Fig. 3. The axes of the frame are frequency (Hz) vs. time (s), by which the variations of harmonic frequencies can be investigated. Fig. 3 shows that the frequencies of harmonics are stationary; they are near to 3rd, 4th and 6th harmonics, but are not integer times of base frequency exactly. The characteristic that the harmonic

frequencies are low implies that the harmonics at PCC point have not any correlations with the PWM harmonics of PV inverters.

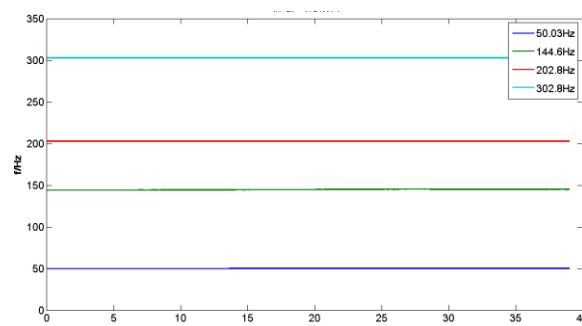


Fig. 3. The frequencies of PCC harmonics over 40s

For waveform recording data, the current waveforms contained harmonics, which were more low times than the harmonics of voltage waveforms in percentages. An additional property should be mentioned is that the voltage and current harmonics are all stationary. The filed tests had been repeated for times at different micro-grid loads and different grouping of the inverters in PV station. The FFT transformation results all indicated that the harmonic components were stationary over 40 seconds.

These field tests and analyses led to the following observations:

- 1) PCC point harmonics are significant, but the micro-grid does not contain any notable harmonic components of voltage and current.
- 2) The harmonics of PV PCC point have no correlation with the PWM frequency.
- 3) Both voltage harmonic and current harmonic exist at the same PCC point; especially, the harmonics are inter-harmonic and leading to the much longer waveform periods than base frequency.
- 4) Although the isolating transformers of PV inverters are Y- Δ topology, triple and even harmonics can exist.

These PCC harmonics cannot be produced by LCL resonance and the behaviors of the inverters in PV station is the main cause for the harmonics. The harmonic distribution in the output circuit of PV inverters has been studied to provide evidence of the harmonic property.

III. INVERTER OUTPUT HARMONIC

One phase output equivalent circuit can be adopted when the output filter of three-phase inverter is symmetrical. The output circuits of PV inverter are depicted in Fig. 4, and the parameters can be found in Table I.

TABLE I
FILTER CIRCUIT PARAMETERS

Parameters symbols	Values
L_o	0.25 mH
C	47 μ F
L_g	0.12 mH (Measured)
R_g	0.01 Ohm (Measured)
V_{grid}	380V(RMS)
V_{DC}	400V

TABLE II

HARMONIC CURRENT AND VOLTAGE IN INVERTER OUTPUT
CIRCUIT

Harmonic component parameters			
$f(\text{Hz})$	144.6	202.8	302.8
$I_{L_o}(\text{A})$	5.47(-70.8°)	40.75(3.6°)	25.99(-23.6°)
$I_{L_E}(\text{A})$	5.58(-70.9°)	42.88(3.3°)	29.56(-23.8°)
$I_C(\text{A})$	0.11(103.8°)	2.14(178.6°)	3.57(154.4°)
$U_C(\text{V})$	0.85(13.8°)	11.90(88.6°)	13.32(64.4°)
$U_{\text{Inverters}}(\text{V})$	2.09(17.0°)	24.86(91.2°)	25.68(65.4°)

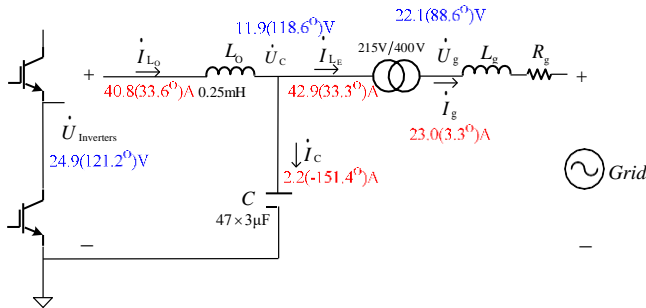


Fig. 4. The output circuit of PV inverter

L_o is filtering inductance; C is filtering capacitor; I_g and R_g are the grid impedance; the ratio of isolating transformer is 400/215. If the transformer ratio is 1 and the grid resistor R_g is zero, the output impedance of grid-connected inverter can be calculated as

$$Z = j\omega \frac{L + L_o - \omega^2 L L_o C}{1 - \omega^2 L_E C} \quad (1)$$

where L_E is the equivalent inductance of the inverter side of isolating transformer. Impedance Z has a resonance frequency related to inductance L_E and filtering capacitor C .

The inductance and capacitor branches of the output circuit of grid-connected PV inverters have frequency responses to harmonics. As an example, considering the 4th harmonic, the calculated node voltages and branch currents in output circuits were depicted in Fig. 4. The blue data are node voltage and the red ones are branch currents of the 4th harmonic; the data in the parentheses are the phase angles of harmonic voltage and current. The harmonic currents of output filter branches satisfy

$$\dot{I}_{L_o} = \dot{I}_{L_E} + \dot{I}_C \quad (2)$$

where I_{L_o} is inverter output harmonic current, I_C is filtering capacitor branch current, and I_{L_E} is the inject harmonic current to grid. The capacitor branch RMS current I_C of the 4th harmonic is 2.2A, which is less 1/15 of the inverter output harmonic current. Voltage $U_{\text{Inverters}}$ is the output harmonic voltage of the inverter IGBT bridge, and whose amplitude is the biggest one in the inverter output circuit. The others harmonic components presented the same distribution behavior of current and voltage in the output circuit. The calculation are depicted in Table II.

All the harmonics listed in TABLE II have the same branch current and node voltage relationships: the harmonic current on filtering capacitor branch is the least one of all current branches with same frequency; the inverter IGBT bridge output harmonic voltage is the most significant one of all node voltages with same frequency. These characteristics can be depicted as:

$$\text{abs} \left(\min \{ I_{L_o}^*, I_{L_E}^*, I_C^* \} \right) = I_C; \quad (3)$$

$$I_C \ll I_{L_o} \text{ \& \& } I_C \ll I_{L_E}$$

$$\text{abs} \left(\max \{ \dot{U}_{\text{Inverters}}, \dot{U}_C \} \right) = U_{\text{Inverters}} \quad (4)$$

The field test and analysis presented some very different results to the LCL resonance. The significant harmonic current branch and highest harmonic voltage node are not related with filtering capacitor branch. These PCC harmonics measured in field are not produced by LCL resonances of inverter output filtering circuits. So, the investigations of harmonics at PCC point of a PV station in a micro-grid should involve the inverter control algorithms, inverter group topology and micro-grid behaviors.

As pointed out in harmonic theory, harmonics due to LCL resonance of inverter output filter usually produce a significant filtering capacitor branch harmonic current, and the filtering capacitor voltage is the highest one of all the node harmonic voltages in the output circuit of an inverter.

In conventional opinion, the PCC point harmonics of grid-connected PV station are usually related to PWM and imperfect current control of inverters. Furthermore, harmonic components of the grid voltage can also lead harmonic amplifications by inverter output filter LCL resonance at PCC point. The frequencies of harmonics are determined by the harmonic sources which excite the harmonic resonances. The harmonic lasting time depend on the harmonic sources' existences. On the contrary, the field measurements indicate that the excitation sources with the frequencies of PCC harmonics do not exist before the resonances take place. The excitation sources should emerge with the harmonic resonances synchronously.

IV. INVERTER OUTPUT IMPEDANCE AND GRID IMPEDANCE

A single-phase grid-connected inverter will remain stable if the ratio of the grid impedance to the inverter output impedance satisfies the Nyquist stability criterion[12]. This criterion is suitable for three-phase inverters when these converters are three-phase symmetric.

The resonance model between the inverter output impedance and the grid impedance can be depicted as below

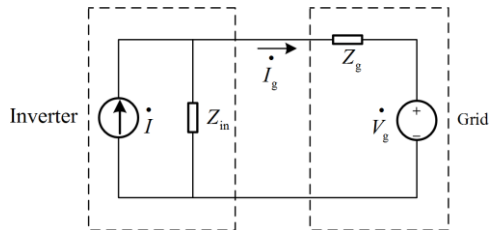


Fig. 5. Resonance model of inverter and grid

where I is the value of an inverter which is working as a current source, Z_{in} is the output impedance of PV inverter, Z_g is the grid impedance, V_g is the grid voltage, and I_g is the current which inverter inject into the grid. The current I_g can be calculated as

$$\dot{I}_g = \dot{I} \cdot \frac{1}{1 + Z_g/Z_{in}} \quad (5)$$

For three-phase inverters, an under-damped resonance will be led if the amplitude ratio of Z_g and Z_{in} is 1 and the phase difference between them is 180° when a harmonic source emerges.

The field test data in this study indicate that the grid-connected inverters and micro-grid are all symmetric even though the frequency components are inter-harmonics, including voltage and current waveforms.

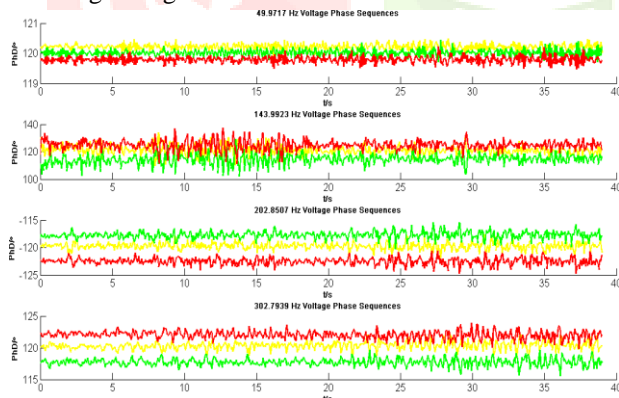
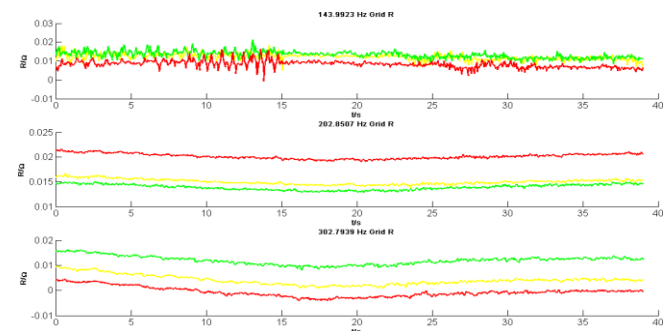


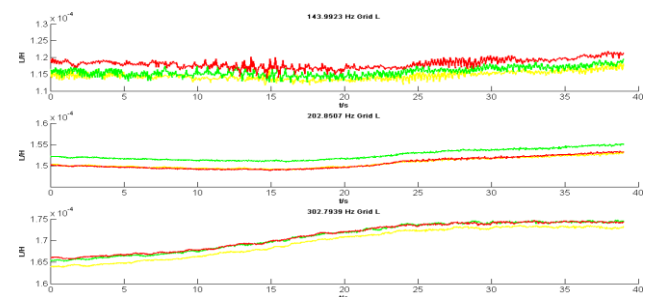
Fig. 6. Phase sequences of fundamental and harmonics

where yellow line is phase A sub. phase B, green line is phase B sub. phase A, and red line is phase C sub. phase A. The phase sequences are near symmetric and the current components have the same phase sequences.

Furthermore, the grid impedances of all harmonics are symmetric. The figures below present the resistance and inductances of harmonic impedance of grid.



(a) Harmonic resistance vs. time



(b) Harmonic inductance vs. time

Fig. 7. Grid Harmonic impedance over 40s

where yellow, green, and red lines are phase A, B and C impedances, respectively. The harmonic resistances are about 0.01 Ohm; the harmonic inductance are about 0.12 mH. These grid impedances vary over time slowly. The properties of harmonics impedances imply that the micro-grid is time-varying, which can be related to the grid load and/or the PV output power variations. And such fluctuations are not necessarily to be measured by the frequency response scanning.

In addition to grid harmonic impedance analysis, the nonlinear properties of PV inverters also impact the PCC point harmonics of PV station. These nonlinear properties of PV inverter involve integral saturation of PI controller, dead-zone of IGBT bridge, and hysteresis loop of isolating transformers.

V. CONCLUSION

High PV penetrations and weak micro-grids lead to PCC point harmonics frequently. This work has implemented field tests and indicated that the causes of these harmonics are very different from conventional harmonics related to LCL resonance or other harmonic amplifications. Inter-harmonic and stationary are two significant characteristics of these PCC harmonics. The analysis of the distributions of harmonic in PV inverter imply that the inverter output impedance and nonlinear properties play an important role in the appearance of PCC point harmonics. The next work should be focused

on the reproductions by simulations and mitigations of PCC harmonics in the weak micro-grid.

ACKNOWLEDGMENT

This work is supported by the National High Technology Research and Development of China 863 Program (2011AA05A106), and the Science and Technology Foundation of State Grid Corporation of China(NYB17201200180).

REFERENCES

- [1] A. Bhowmik, A. Maritra, S. M. Halpin, and J. E. Schatz, "Determination of allowable penetration levels of distributed generation resources based on harmonic limit considerations," *IEEE Transactions on Power Delivery*, vol. 18, no. 2, pp. 619–624, 2003.
- [2] O. Vodyakho and C. C. Mi, "Three-level inverter-based shunt active power filter in three-phase three-wire and four-wire system," *IEEE Trans. Power Electron.*, vol. 24, no. 5, pp. 1350–1363, May 2009.
- [3] K. H. Ahmed, A. M. Massoud, S. J. Finney, and B.W. Williams, "A modified stationary reference frame-based predictive current control with zero steady-state error for LCL coupled inverter-based distributed generation systems," *IEEE Trans. Ind. Electron.*, vol. 58, no. 4, pp. 1359–1370, Apr. 2011.
- [4] K. N. M. Hasan, K. Rauma, P. Rodriguez, J. I. Candela, R. S. Munoz-Aguilar, and A. Luna, "An overview of harmonic analysis and resonances of large wind power plant," in *Proc. IECON 2011*, pp. 2467–2474, 2011.
- [5] J. He, Y. W. Li, and S. Munir, "A flexible harmonic control approach through voltage controlled DG-grid interfacing converters," *IEEE Trans. Ind. Electron.*, vol. 59, no. 1, pp. 444–455, Jan. 2011.
- [6] Q. Zeng and L. Chang, "An advanced SVPWM-based predictive current controller for three-phase inverters in distributed generation systems," *IEEE Trans. Ind. Electron.*, vol. 55, no. 3, pp. 1235–1246, Mar. 2008.
- [7] E. Wu and P.W. Lehn, "Digital current control of a voltage source converter with active damping of LCL resonance," *IEEE Trans. Power Electron.*, vol. 21, no. 5, pp. 1364–1373, Sep. 2006.
- [8] G. Shen, X. Zhu, J. Zhang, and D. Xu, "A new feedback method for PR current control of LCL-filter-based grid-connected inverter," *IEEE Trans. Ind. Electron.*, vol. 57, no. 6, pp. 2033–2041, Jun. 2010.
- [9] J. C. Wiseman and B. Wu, "Active damping control of a high-power PWM current-source rectifier for line-current THD reduction," *IEEE Trans. Ind. Electron.*, vol. 52, no. 3, pp. 758–764, Jun. 2005.
- [10] B. Badrzadeh and M. Gupta, "Power system harmonic analysis in wind power plants - part II: experiences and mitigation methods," in *Proc. IEEE IAS 2012 Annual Conference*, pp. 1–8, 2012.
- [11] Y. W. Li, "Control and resonance damping of voltage source and current source converters with LC filters," *IEEE Trans. Ind. Electron.*, vol. 56, pp. 1511–1521, May 2009.
- [12] X. Chen and J. Sun, "A study of renewable energy system harmonic resonance based on a DG test-bed," in *Proc. IEEE APEC 2011*, pp. 995–1002, Ft. Worth, TX, March 2011.

